

# Final Results of the TerraSAR-X In-Orbit Antenna Model Verification

Markus Bachmann, Marco Schwerdt, Benjamin Bräutigam, Björn Döring

German Aerospace Center (DLR), Oberpfaffenhofen, 82234 Weßling, Germany,

Tel: 08153 28-2395, Fax: 08153 28-1449

markus.bachmann@dlr.de

**Abstract**— TerraSAR-X is a highly flexible X-band radar satellite. Its primary objective is the acquisition of high quality SAR images in a multitude of possible acquisition modes. The great amount of antenna patterns needed for image acquisition and correction requires an antenna model accurately describing all beams. To guarantee the required image quality, the model was verified in-orbit during the commissioning phase following the launch in June 2007. The methodology of the antenna model verification as well as the final results obtained are presented in detail in this paper.

## I. MOTIVATION

TerraSAR-X is a versatile X-Band SAR satellite built in a Public Private Partnership between DLR and Astrium. The main payload of TerraSAR-X is a synthetic aperture radar instrument to acquire high quality radar images of the Earth's surface.

### A. Instrument specification

The radar instrument comprises an active phased array antenna which allows flexible beam forming. The antenna characteristics can be accurately modelled by mathematical equations based on on-ground measurements. The antenna with its 4.8 m length and 0.7 m width consists of 384 slotted wave-guides arranged in 12 panels in azimuth direction (columns) each with 32 subarrays (rows) [1]. The nominal antenna pointing in elevation is 33.8° away from nadir. Right and left looking acquisition is realised by satellite roll manoeuvres. Each individual subarray is driven by transmit-receive modules (TRMs) adjustable in amplitude and phase by applying complex excitation coefficients. This enables beam steering and adaptive beam forming in both azimuth and elevation direction. For the multitude of standard acquisition modes possible on TerraSAR-X - like nominal Stripmap, ScanSAR or Spotlight - and the several experimental modes - like quad-pol mode, wide band operation or along-track interferometry - more than 10 000 different beams can be commanded.

### B. Antenna model application

This great amount of beams and modes is one highlight but also a great challenge of the whole mission and the main driver for the need of an accurate antenna model. The model is primarily used to generate the antenna patterns needed by the processing system to correct for the antenna characteristic of each beam. The antenna characteristic is mapped into the acquired SAR signal as the reflection of the ground is overlaid by the gain pattern of the antenna in range. In azimuth, the

pattern is contained in the Doppler spectrum and hence needed for correct Doppler estimation.

A second important reason for the antenna model is the optimisation of the beam excitation coefficients prior to launch to achieve an optimum performance for the full performance beams in terms of Noise Equivalent Sigma Zero (NESZ) and Total Ambiguity Ration (TAR).

## II. ANTENNA MODEL THEORY

The antenna model calculates radiation patterns by superposition of measured embedded subarray patterns weighted by beam excitation coefficients considering the exact geometrical dimensions of the antenna.

For cuts in elevation and azimuth the radiated pattern  $F_{Beam}$  is calculated by [2]

$$\bar{F}_{Beam}(\varepsilon, \alpha) = \sum_{m=0}^{M-1} \sum_{n=0}^{N-1} (\bar{C}_{SA, mn}(\varepsilon, \alpha) \cdot a_{mn} \cdot E_{SA, mn} \cdot e^{jk \sin \varepsilon \cos \alpha \left( \frac{N-1}{2} + n \right) \Delta y} \cdot e^{jk \cos \varepsilon \sin \alpha \left( \frac{M-1}{2} + m \right) \Delta x})$$

with the desired elevation and azimuth angle  $\varepsilon$  and  $\alpha$ , the amount of subarrays in  $N$  rows and  $M$  columns, the inter-subarray distances  $\Delta x$  (columns) and  $\Delta y$  (rows) and the wave number  $k$ .

The embedded subarray patterns  $C_{SA}$  describe the radiation characteristics of the individual subarray elements embedded into the whole antenna and have to be given for each row, column, elevation and azimuth angle. The commanded complex excitation coefficients are given by  $a$ . Finally, the error matrix  $E_{SA}$  describes drifting or failed antenna elements which are determined via internal calibration loops and orthogonal code sequences applied to the TRMs [3].

The TerraSAR-X operation and calibration approach requires a very high accuracy of the antenna model. Hence, the antenna model has to reproduce the behaviour of the real antenna as exact as possible. Therefore, accurately measured characterisation data i. e. embedded subarray patterns are used. These measurements were performed by the Astrium GmbH in the Planar Near Field Scanner (PNFS).

## III. ANTENNA MODEL STRATEGY

As denoted before, the development of the antenna model was driven by three main requirements:

- The great number of more than 10,000 different beams to be calibrated
- The tight performance requirement of an overall radiometric accuracy goal of better than 1 dB. From this requirement the accuracy for the antenna model of better than 0.2 dB for reproducing the pattern shape and predicting the absolute gain was derived.
- The desired short duration of the commissioning phase.

To ensure these requirements, several steps were realized:

- As much effort as possible was moved from in-orbit tasks to on-ground duties. This includes the accurate measurement of the embedded subarray patterns as well as the validation of the model on-ground before launch. This was done by comparing modelled patterns with measured patterns. This was successfully performed by Astrium and DLR, showing a first confidence on the excellent performance of the antenna model [4].
- Different in-orbit calibration techniques for antenna model verification and a sufficiently high amount of measurements, in case of TerraSAR-X over two hundred measurements were executed. Therefore, in-orbit verification was performed during the commissioning phase in the first months after launch. The verification can be divided into three main tasks:
  - measurements across the rainforest to verify the elevation pattern shape
  - the use of ground receivers to verify the azimuth pattern and
  - ScanSAR measurements over rainforest and over ground receivers to verify the calculated beam-to-beam gain variation
- To ensure a short commissioning phase, the verified antenna model was used to support the radiometric calibration as well as for pointing calibration [6].

#### IV. IN-ORBIT VERIFICATION RESULTS

##### A. Antenna Model Verification in Elevation

In elevation, the simulated relative antenna patterns are compared with estimated patterns. The estimates are extracted from SAR images acquired over rainforest in the Amazon basin, Brazil (see upper image in Figure 1). Amazon rainforest is a quite homogeneous scatterer and the pattern shape is clearly visible in the SAR raw data. However, as this raw data consist of pulses without any processing, the image processed in the nominal SAR processor is used for pattern estimation. In the processing chain, the accurate position and geometry of the acquisition is determined and annotated after azimuth and range compression. Then the antenna patterns mapped in the image data are corrected with the available modelled reference antenna patterns [5].

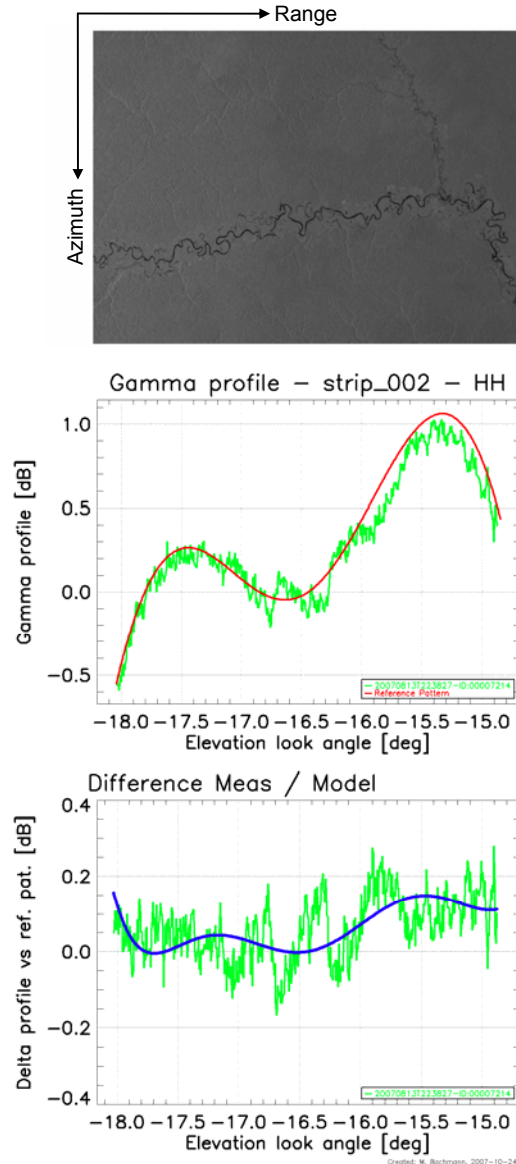


Figure 1: Comparison between the range profile (green points) of the upper rain forest scene versus the reference elevation pattern (red line) in the middle figure, deviation between both and fit in the lower figure.

For pattern estimation, this pattern correction has to be reversed with the used reference patterns to obtain the original antenna characteristics in the image. Then, the image is freed from disturbances like rivers or de-forested areas using an automatic masking algorithm. The radar image is denoted in beta nought  $\beta_0$  where the backscatter depends on the incidence angle  $\theta$ . For the comparison however, the gamma nought  $\gamma_0$  has to be derived via the sigma nought  $\sigma_0$  using the formula [7]:

$$\gamma^0 = \sigma^0 / \cos(\theta) = \beta^0 \cdot \tan(\theta)$$

Finally all azimuth lines are summed up and the pixel-elevation angle transformation is applied to obtain the so called Gamma Profile which is a vector of the mean antenna pattern over elevation angle.

An exemplary result is depicted in the middle part of Figure 1. The noisy ripple is the gamma profile, which now can be compared to the modelled reference pattern depicted in red.

The described evaluation was performed for a huge number of acquisitions in different beams and polarisations. The results show a quite excellent accordance between the simulated antenna pattern and the measured gamma profiles. The deviation and hence the accuracy of the antenna model is below  $\pm 0.2$  dB peak-peak. This can be seen in the lower part of Figure 1 where the deviation between the reference antenna pattern and the estimated pattern is depicted for the exemplary beam. Additionally, by fitting a curve into the profile, a noise-free picture can be obtained.

### B. Antenna Model Verification in Azimuth

Although the algorithm used in the antenna model for calculating the antenna patterns is equal for elevation and azimuth pattern calculation, both directions were verified to ensure the antenna model quality and by this checked for eventual deviations in the underlying components like power dividers or amplifiers.

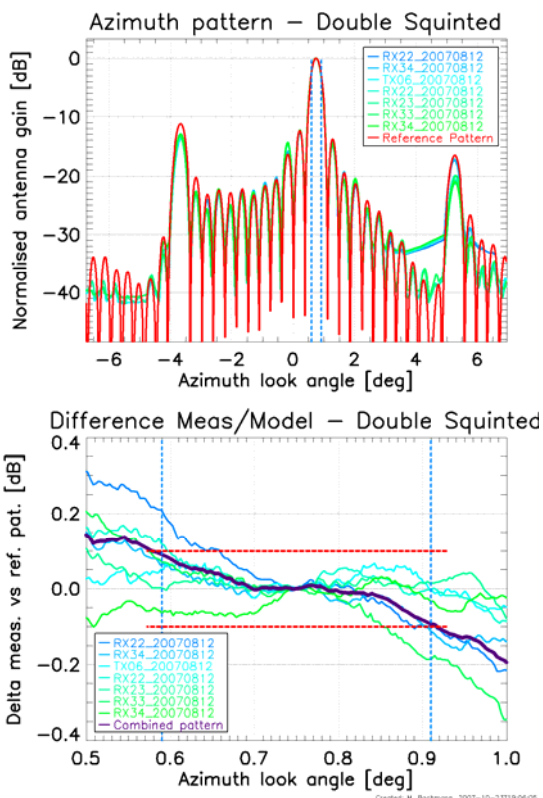


Figure 2. Transmit patterns compared to a reference pattern (upper figure) and their deviation.

The verification of the antenna pattern in azimuth direction was performed for transmit pattern only using the DLR ground calibration equipment in form of ground receivers [9]. These receivers record the amplitude of the pulses transmitted by the SAR antenna. Transformed to the antenna elevation angles and corrected by position information, the azimuth

antenna pattern is obtained and can be compared to the modelled pattern. The measurements were performed for patterns over the whole specified angular range of the SAR antenna with ground receivers placed at the near, mid and far range within the swaths.

Figure 2 shows the special case of a double squinted beam. This is a beam steered to angles of  $+0.75^\circ$  in azimuth and  $-16.5^\circ$  in elevation which is at the specified limits for antenna steering. Again, the reference pattern generated by the model is depicted in red, the measured antenna patterns in green to blue. The measured patterns are quite smooth which results from an averaging over several independent pulses. As for elevation, the antenna model verification shows extraordinary results. The resulting deviation within the 3 dB beamwidth for one pass as shown in purple in the lower part of Figure 3 is less than  $\pm 0.1$  dB. This is half of the nominal requirement as only the one-way pattern is measured with ground receivers.

### C. Verification of the Beam-to-Beam Gain Variation

Besides the verification of the pattern shape, the beam-to-beam gain prediction capability of the antenna model is of great importance. First, this is required for the ScanSAR processing, where four different beams with different antenna gains are acquired, corrected with their corresponding pattern and combined into one image. Second, with an appropriate gain prediction, only one Absolute Calibration Factor can be derived for the complete system [8].

The beam-to-beam gain prediction is verified evaluating ScanSAR data. In ScanSAR acquisitions, the beam is switched sequentially from burst to burst between the four neighbouring swaths to get a broader swath width than for normal Stripmap acquisitions. By generating the unnormalised gamma profile for each of the four swaths, the relative gain deviation can be determined. In Figure 3, several of these ScanSAR evaluations for different beams have been combined in one diagram to show the gain prediction over a wide angular region. As the images were acquired over different parts of the rainforest with different vegetation types and hence different backscatter, each complete ScanSAR acquisition was connected to their predecessor within the overlapping regions. The upper part of Figure 3 shows the gamma profiles versus reference pattern, the plot in the middle depicts the deviation between pattern and profile. The lower part shows the deviation between the overlapping regions of two ScanSAR swaths of one acquisition. The results again have an excellent performance of below  $\pm 0.2$  dB peak-peak except one area where a heavy thunderstorm disturbed the acquisition.

A second method of gain variation verification was performed by placing a ground receiver in the swath overlapping region of two swaths and recording transmit azimuth pattern. In the received pulses, the switching between the four ScanSAR beams is clearly visible in Figure 4. The deviation between the overlapping beams can be compared with the antenna model and even here as above, the deviation is within the expected values.

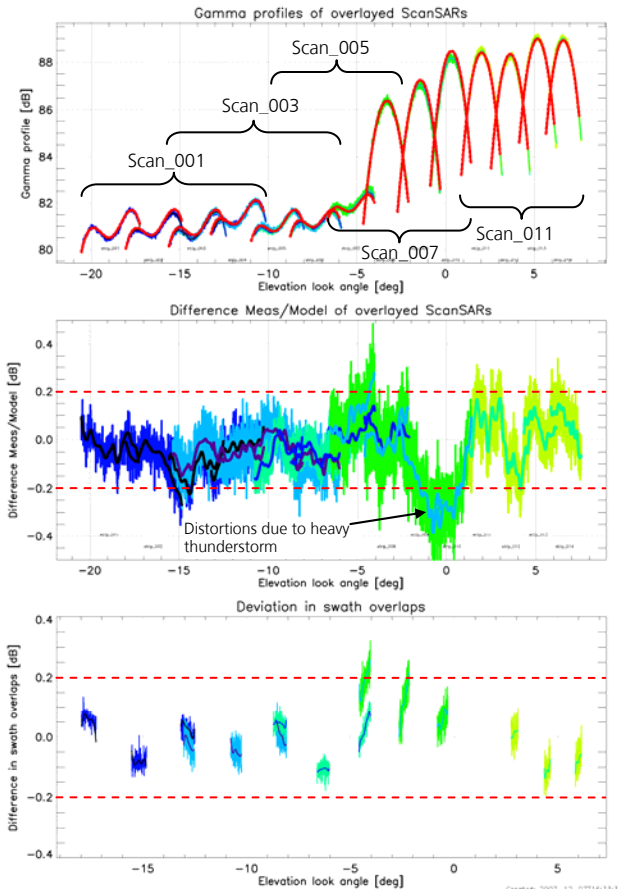


Figure 3 Beam-to-beam gain verification using ScanSAR images.

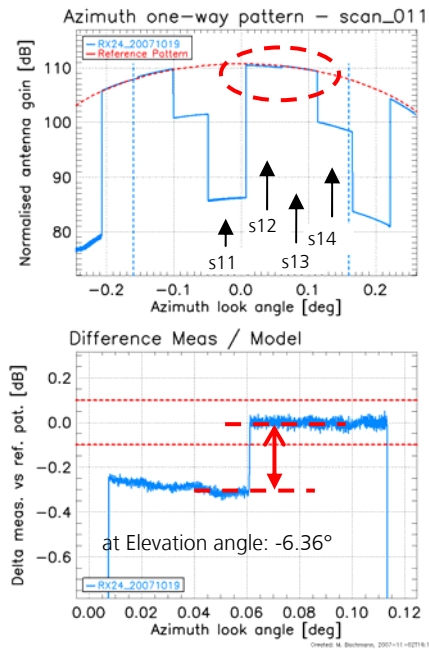


Figure 4 Beam-to-beam gain verification using ground receivers.

## V. COMMISSIONING PHASE SUPPORT

Finally, the verified antenna model helps to ensure a short commissioning phase [6]. Both the pointing calibration and the determination of the absolute calibration factor will be supported by the antenna model.

The antenna model was used to generate Notch patterns for pointing calibration. By pointing calibration it is ensured that the main radiation beam of the antenna looks in the desired direction in elevation. In azimuth, especially the difference between geometric and estimated Doppler centroid, applying a Doppler Estimator to the acquired raw data, was evaluated in order to minimize their deviation.

With the properly working antenna model, the absolute calibration factor, i.e. the equivalent radar backscatter coefficient of targets, does not have to be measured for all relevant beams. It is measured for one beam and verified by several representative beams, hence again verifying the antenna model itself [8]. By this verification approach it is possible to shorten the time and the effort for the absolute radiometric calibration during the commissioning phase as the absolute calibration factor of only a few of the 10,000 beams have to be measured.

## VI. CONCLUSION

The TerraSAR-X antenna model is utilised for generating the reference antenna patterns for processing and for beam optimisation. To ensure the specified product quality, its accuracy has been verified in orbit during the commissioning phase following the TerraSAR-X launched in June 2007. The results show the excellent performance of both, the TerraSAR-X satellite itself and the antenna model, which was verified on providing the reference antenna patterns with an accuracy of better than  $\pm 0.2$  dB.

## ACKNOWLEDGEMENT

A great thank is dedicated to the whole TerraSAR-X team and especially to the HR calibration team for supporting the antenna model verification with an uncountable number of calibration campaigns and their unwearied effort at every possible weather and environmental conditions.

## REFERENCES

- [1] R. Werninghaus, S. Buckreuss, W. Pitz: "TerraSAR-X Mission Status" *Geoscience and Remote Sensing Symposium, IGARSS*, Barcelona, Spain, July 2007
- [2] B. Grafmüller, A. Herschlein, C. Fischer: The TerraSAR-X Antenna System; *Radar Conference, IEEE International*, May 2005
- [3] B. Bräutigam, J. Hueso González, M. Schwerdt, M. Bachmann: Radar Instrument Calibration of TerraSAR-X, *7<sup>th</sup> European Conference on Synthetic Aperture Radar*, Friedrichshafen, Germany, June 2008
- [4] M. Bachmann, M. Schwerdt, B. Bräutigam, B. Grafmüller, A. Herschlein, J. L. Álvarez-Pérez: The TerraSAR-X Antenna Model Approach; *Proceedings on INICA 07*, Munich, Germany, March 2007
- [5] J. L. Álvarez-Pérez, M. Schwerdt, M. Bachmann: TerraSAR-X Antenna Pattern Estimation by Complex Treatment of Rain Forest Measurements; *Geoscience and Remote Sensing Symposium, IGARSS 2006*, Denver, USA, July 2006
- [6] M. Schwerdt, D. Hounam, J. L. Alvarez-Pérez: The calibration concept of TerraSAR-X: a multiple-mode, high-resolution SAR, *Canadian Journal of Remote Sensing*, Vol. 31, No. 1, pp. 30-36, 2005
- [7] J. E. Laycock, H. Laur: ERS-1 SAR Antenna Pattern Estimation - ES-TN-DPE-OM-JL01, iss. 1, rev. 1, September 1994, [http://earth.esa.int/ers/instruments/sar/sar\\_AP\\_est/](http://earth.esa.int/ers/instruments/sar/sar_AP_est/)
- [8] M. Schwerdt, B. Bräutigam, M. Bachmann, B. Döring, J. Hueso-Gonzalez, D. Schrank: Final Results of the Efficient TerraSAR-X Calibration Method, *IEEE Radar Conference*, Rome, Italy, May 2008
- [9] B. Döring, M. Schwerdt, R. Bauer: TerraSAR-X Calibration Ground Equipment, *Proceedings of WFMN07*, Chemnitz, Germany, 2007